Image Preprocessing of Fingerprint Images Captured with a Mobile Camera

Sanghoon Lee, Chulhan Lee, and Jaihie Kim
Department of Electrical and Electronic Engineering,Yonsei University
Biometrics Engineering Research Center, Seoul, Korea

***Abstract*— In this paper, we introduce the recognition of fingerprint images captured with a mobile camera. The corresponding image preprocessing algorithms are also discussed. Some characteristics of fingerprint images captured with mobile cameras are quite different from those obtained by conventional touch-based sensors. For example, mobile camera images are colored while conventional touch-based sensors produce only black and white images. Also, the backgrounds, or non-finger regions, in mobile camera images are very erratic depending on how the image captures place and time. Images from conventional sensors always display uniform background regions which are very different from the fingerprint regions. Thus for the segmentation of the fingerprint regions from the background regions, we use not only texture information but also color and size information. The information on ridge orientations in fingerprint images is useful in most noise elimination and thinning processes, and the gradient-based approach is used typically for these processes. However, because the gradient-based approach is very weak at the outliers and because mobile cameras produce more noise than conventional sensors, we propose a robust regression method that removes the outliers iteratively and effectively. In the final preprocessing stage, we divide the fingerprint images into small blocks and estimate the quality of each image in terms of good or bad quality regions. This estimation is based on the consistency among the sub-block images, and bad regions are discarded in the later feature extraction stage. If the quality is too poor, then the whole image is rejected. Our experiments show that the proposed preprocessing algorithms produce better results than the conventional ones when they are applied to images captured by a mobile camera.**

***Index Terms*— On-line Fingerprint verification, minutiae, Quality measurement, Orientation estimation.**

I. Introduction

Mobile products are used in various applications such as communication devices, digital cameras, schedule management devices, and mobile banking. Due to the proliferation of these products, privacy protection is becoming more important in today's world. The security of these mobile devices has depended mainly on passwords up until the present day. This presents the serious problem of password robbery or surreptitious use.

Biometric recognition refers to the use of distinctive physiological and behavioral characteristics (e.g. fingerprint, face, iris, and hand geometry) to automatically recognize a person. Among these, fingerprint recognition has been the most widely exploited because of stability, usability, and low cost. For fingerprint recognition technology to be applied to mobile security devices, an additional fingerprint sensor is necessary when manufacturing these devices. This leads to weakening durability and increasing price. Fortunately, almost all modern mobile products are already equipped with color cameras. These cameras are comparable in quality to commercial digital cameras, because they possess such features as zooming, autofocusing, and high resolution. There are challenging problems when developing fingerprint recognition systems that use a mobile camera. First, the contrast between the ridges and the valleys in images obtained with a mobile camera is low. Second, because the depth of field of the camera is small, some parts of the fingerprint regions are in focus but some parts are out of focus. Third, the backgrounds, or non-finger regions, in mobile camera images are very erratic depending on how the image captures place and time.

In this paper, we propose a preprocessing algorithm for fingerprint images captured with a mobile camera. In the following section, we describe this preprocessing algorithm. Section 2 explains the segmentation algorithm. Section 3 presents the orientation estimation that is robust to noise. Section 4 presents the quality estimation algorithm. Experimental results are shown in section 5, followed by a conclusion in section 6.

II. Fingerprint Segmentation

After acquiring a fingerprint image with a mobile camera, the first step is fingerprint segmentation. This divides the input image into a foreground (fingerprint) region and a background region. When a fingerprint image is obtained from an existing sensor (touch-based sensors such as capacity, optical, thermal sensors, etc.), the background region has similar patterns depending on the sensor type. This makes it easy to segment the fingerprint region. When a fingerprint is captured by a mobile camera, the image background region is very erratic depending on how the image captures place and time. Fig. 1 shows the input fingerprint images of three types of sensors. We segment the fingerprint region with the following information:

i) Color information: the color of all human fingerprints is similar.

ii) Texture information: when the fingerprint is acquired from the camera, a close-up shot is needed. This leads to a reduced depth of field (Dof). So, the fingerprint region shows a clear pattern but the background region shows a blurred pattern.

iii) Size information: the fingerprint region is the largest object in an input image.

The results of segmentation through color and texture information are combined and the largest region in the combined image is extracted.

A. Fingerprint Segmentation Using Color Information

There have been many on-going and past efforts in the study of object segmentation using color information[1][2]. In order to segment fingerprint regions using color, we compare each pixel of the input image with the distribution of the fingerprint color model in a color space. The fingerprint color model is created as a Gaussian PDF with supervised learning. The overall procedure for designing the fingerprint color model is as follows:

i) Create training images by manually separating the fingerprint regions.

ii) Transform the color values of the fingerprint regions into the normalized color space.

iii) Estimate the parameters(mean and covariance) of the color distribution.

We produced 200 training images and 600 test images. One of the training images is shown in Fig. 2 Because the primary color space (RGB) is influenced by illumination, all the color information in the fingerprint region has been converted to the normalized color space. The transform equation from the RGB color space to the normalized color space is r=R/(R+G+B), g=G/(R+G+B), b=B/(R+G+B) where R, G, B are Red, Blue and Green in the RGB space and r, g, and b are the normalized three components of the normalized color space. Since the three normalized color components are linearly dependent (r+g+b=1), only two components are used for the fingerprint color model. Fig. 3 shows the distribution of the fingerprint color model in the normalized color space. Based on the normalized color value, a fingerprint color model represented by a 2D Gaussian model $N(\mathbf{m}, \mathbf{\Sigma}^2)$ is obtained, where is obtained, where $\mathbf{m} = (\bar{r}, \bar{b})$with

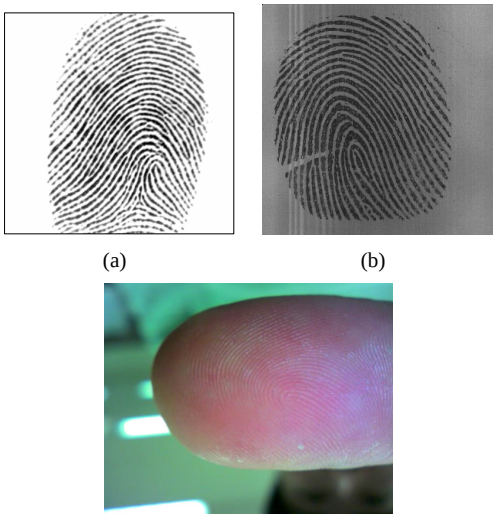

(a) (b) (c)

Fig. 1. Fingerprint Images: (a) Optical Sensor (b) Capacitive Sensor (c) Mobile Camera

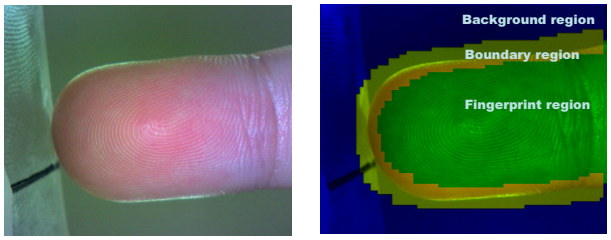

(a) (b)

Fig. 2. Training Images: (a) Original image (b) Manually segmented image

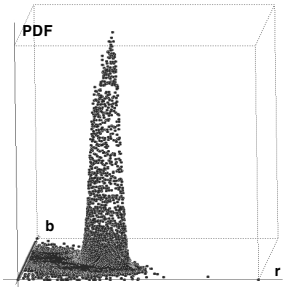

Fig. 3. The distribution of the fingerprint color model

$\bar{r} = \frac{1}{N}\sum_{i=1}^{N} r_i$, $\bar{b} = \frac{1}{N}\sum_{i=1}^{N} g_i$, and $\mathbf{\Sigma} = \begin{bmatrix} \sigma_{rr} & \sigma_{rb} \\ \sigma_{br} & \sigma_{bb} \end{bmatrix}$.

The Mahalanobis distance ($D(i)$) between the 2D Gaussian fingerprint color model and each pixel $\mathbf{x}(i)$ of the input image is measured as follows:

$$D(i) = (\mathbf{x}(i) - \mathbf{m})^T \Sigma^{-1} (\mathbf{x}(i) - \mathbf{m}) \quad (1)$$

where m is the mean vector of the fingerprint color model and $\sum$ is the covariance matrix. If the Mahalanobis distance is less than a threshold Tc, the pixel is regarded as part of the background region, otherwise the pixel is regarded as part of the foreground region. The Tc is defined experimentally.

B. Fingerprint Segmentation Using Texture Information

A close-up shot is required to capture the fingerprint image. This makes the depth of field (Dof) small. Therefore, the fingerprint region is in focus and the background region is out of focus. This produces clear ridge-pattern images in the fingerprint region and blurred-pattern images in the background region. Our method is based on DWT (Discrete Wavelet Transform) which is widely exploited in texture segmentation and classification [3][4].

The proposed algorithm consists of three steps: wavelet decomposition, feature extraction and segmentation. In wavelet decomposition, using Daubechies' 9/7 filter, a gray-value image converted by averaging the color components (RGB) is decomposed into three levels. Fig. 4(a) shows the three level wavelet decomposition of an input image. The goal of feature extraction is to obtain a set of measures which can be used to discriminate between the fingerprint region and the background region. Our features are calculated in the detail images of the third level wavelet domains (Fig. 4(a): 2),3),4))

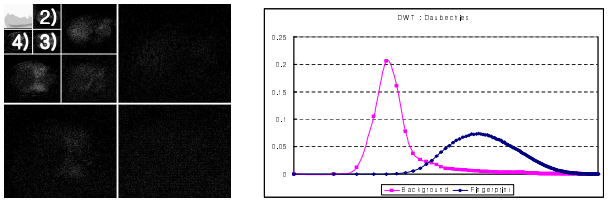

(a) (b)

Fig. 4. (a) The wavelet domain of a fingerprint image (b) The distribution of features

as follows:

$$F(i,j) = \frac{1}{3}\sum_{h=2}^{4} s_h(i,j)$$
$$s_h(i,j) = \frac{1}{(2n+1)^2}\sum_{k=i-n}^{i+n}\sum_{l=j-n}^{j+n}|g(k,l) - m(i,j)| \quad (2)$$

where is a absolute deviation over a window of size (2n+1)×(2n+1), g(k,l) is the wavelet coefficient and $m(i,j)$ is the mean of the window. Fig. 4(b) shows the distribution of the feature values of the fingerprint region and the background region with manually segmented images (the training images in section 2.1). The distribution shows that the feature values of the background region are concentrated on low value and the feature values of fingerprint region spread out wildly. Taking advantage of this characteristic, segmentation is achieved through the simple threshold method.

C. Combining the Color and Contrast Information

The final fingerprint segmentation algorithm is accomplished by combining the two sets of results obtained with color (section 2.1) and with texture (section 2.2). We combine the results with the AND operator. After combining, the largest candidate fingerprint region in the combined image is selected through a labeling algorithm, and morphological processing is executed to remove the noise. Fig. 5 shows the resulting images of color, contrast, combining, and final segmentation. In the section 5, the proposed segmentation algorithm is evaluated by manually segmented images.

III. Fingerprint Orientation Estimation

The ridge orientation of fingerprint images plays an important role in fingerprint recognition systems such as singular point detection, ridge enhancement, and fingerprint classification. Many algorithms have been proposed for orientation estimation, which include gradient-based approaches [5][6][7][8], model-based approaches [9][10], filter bank-based approaches [11], and image-based approaches [12]. Among these, the gradient-based approaches are the most popular because of low computational complexity. The gradient-based approaches are very sensitive to noise, non-white Gaussian noise in the gradient field. In this section, we discuss the gradient-based approach and then a new orientation estimation approach based on robust regression is proposed.

A. Gradient-Based Orientation Estimation

The gradient-based approach extracts the dominant ridge orientation in the gradient field of a sub-block image using least squires method, which is equal to the first eigenvector of the PCA in the gradient field[7]. A fingerprint image is divided into sub-blocks, and the horizontal and perpendicular gradients are computed by the Sobel operator. The orientation of the sub-block is computed by:

$$\hat{\theta} = \frac{1}{2}\mathrm{atan}\left(\frac{\sum_{i=0}^{N-1} 2\mathrm{G}_{x_i}\mathrm{G}_{y_i}}{\sum_{i=0}^{N-1}\mathrm{G}_{x_i}^2 - \mathrm{G}_{y_i}^2}\right) + \frac{\pi}{2} \quad (3)$$

where G_{x_i} and G_{y_i} denote the horizontal and perpendicular gradients within a sub-block. Fig. 6 shows the part of the fingerprint region and the corresponding gradient field. The orientation of the dominant gradient, a line shown in Fig. 6(b), is alternatively modeled by the following equation:

$$y_i = \hat{\beta}x_i + \varepsilon_i \quad (4)$$

where x_i and y_i are G_{x_i} and G_{y_i} respectively, and ε_i is error. The simplest method to calculate $\hat{\beta}$ is with the Least Squires (LS) method:

$$\hat{\beta} = (\mathbf{X^T X})^{-1}\mathbf{X^T Y} \quad (5)$$

where $\mathbf{X} = [x_1, x_2, ..., x_n]$ and $\mathbf{Y} = [y_1, y_2, ..., y_n]$.
The LS method finds the optimal answer when the distribution of error ε is white Gaussian ($E(\varepsilon) = 0$, $Var(\varepsilon) = \sigma^2 I$). However, we cannot consider ε as white Gaussian in practical cases. This non-white Gaussian noise tends to generate "outliers", and these outliers may have a strong influence on the method of least squares [13]. Fig. 7 shows the effects of the outliers in the LS method.

B. Orientation Estimation Based On the Iterative Robust Regression Method

As mentioned above, the outliers produce a strong effect on the orientation estimation if the Least Squares method is

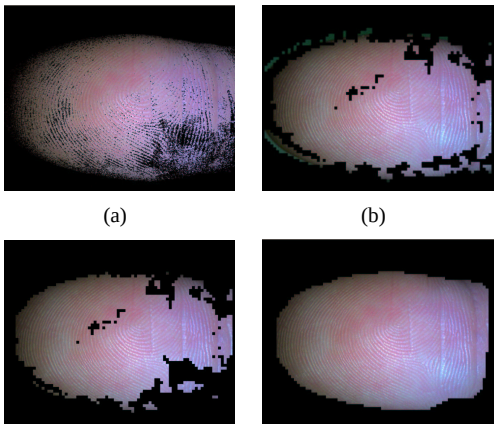

(a) (b)

(c) (d)

Fig. 5. The resulting images: (a) Color (b) Contrast (c) Combining (d) Final result

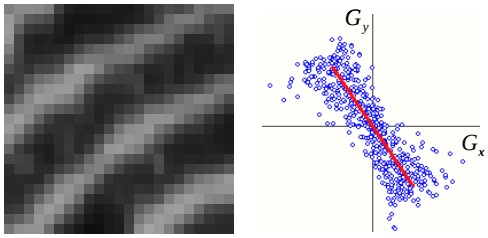

Fig. 6. The fingerprint region and a gradient field: (a) Fingerprint region (b) Gradient field

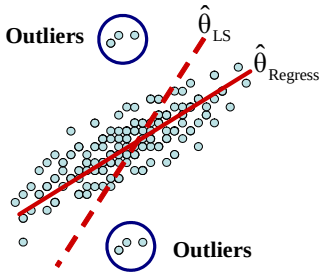

Fig. 7. Effect of outliers in orientation estimation

used. In fingerprint images captured with a mobile camera, the outliers are caused by scars of fingerprints and camera noise. To overcome the problem of outliers, the robust regression method is exploited. This method tends to leave the residuals associated with the outliers. In addition to insensitivity to the outliers, a robust estimation method should produce essentially the same results as the LS method when the underlying distribution is normal and there are no outliers. In our proposed algorithm, we assume that the gradient elements corresponding to the ridges are major to those corresponding to the outliers in the gradient filed. The flowchart of the proposed orientation estimation algorithm is shown in Fig. 8. The main steps of the algorithm include:

i) 2-Dimensional gradients ($\mathbf{x}_i = [G_x, G_y]$): An input image is divided into sub-blocks, and the 2-Dimensional gradients are calculated using the Sobel operator.

ii) Orientation estimation: Using the calculated 2-Dimensional gradients, the orientation of the sub-block is estimated by the LS method.

iii) Whitening: The gradients ($\mathbf{x}_i$) are whitened to measure a norm in the Euclidean space [14].

iv) Removing the outlier: In the whitened 2-Dimensional gradients, a gradient is removed if the Euclidean norm of the whitened gradient ($\|\mathbf{x}_i\|_w$) is larger than 2σ , where σ is 1 because of whitening.

v) Orientation re-estimation: Using the 2-Dimensional gradients from step 4, the orientation ($\theta(n+1)$) of the sub-block is re-estimated by the LS method.

vi) Iterative procedure: If $|\theta(n+1) - \theta(n)|$ is less than Th, the procedure is stopped. If not, we revert to step 3. The Th is defined experimentally.

In the whitening step, the 2-dimensional gradient field is

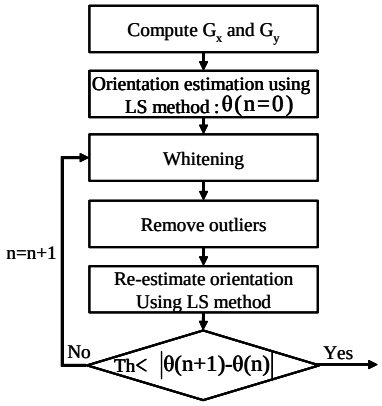

Fig. 8. The overall procedure of the proposed approach

whitened by:

$$\begin{aligned} \mathbf{E^{-1}}\varepsilon &= \mathbf{E^{-1}Y} - \mathbf{E^{-1}X}\beta \\ Cov(\mathbf{X},\mathbf{Y}) &= \mathbf{\Sigma} = \mathrm{E^T E} \end{aligned} \tag{6}$$

where X is $[x_1, x_2, ..., x_n]$, Y is $[y_1, y_2, ..., y_n]$, and ε is noise. The norm of the noise is calculated as:

$$\left\|\mathrm{E}^{-1}\varepsilon\right\|_2 = \varepsilon^T\Sigma^{-1}\varepsilon = (Y - X\beta)^T\Sigma^{-1}(Y - X\beta) \tag{7}$$

Since the gradient elements corresponding to the outliers have an influence on the orientation estimation, the gradient elements corresponding to the outliers have relatively larger Euclidean norm values than those corresponding to the ridges in the whitened gradient field. So, the gradient elements corresponding to the outliers are removed by comparing the norms of the gradient elements as follows:

$$x_i = \begin{cases} x_i & \text{if } \|x_i\|_{\mathrm{w}} < 2\sigma \\ 0 & \text{otherwise} \end{cases} \tag{8}$$

where $\|x_i\|_{\mathrm{w}}$ is a Euclidean norm of the whitened gradient element.

The noise can be modeled by:

$$\begin{gathered} \varepsilon = \sum_{\mathrm{i=1}}^{\mathrm{n}} \varepsilon_{\mathrm{i}} \\ \mathrm{E}(\varepsilon_{\mathrm{k}}) = 0,\ \mathrm{Var}(\varepsilon) = \sigma^2\mathbf{V} = \sum_{\mathrm{i=1}}^{\mathrm{n}} \sigma_{\mathrm{i}}^2\mathbf{V}_{\mathrm{i}} \\ \sigma_{\mathrm{k}}^2 > \sigma_{\mathrm{k-1}}^2\,(\,\sigma_{\mathrm{n}}^2 \approx 0) \end{gathered} \tag{9}$$

where V_{k} is the nonsingular positive symmetric matrix, and σ_k is the variance of noise. Removing the outlier iteratively, the gradient elements corresponding to the largest variance($\sigma_k > \sigma_{k-1} > \sigma_{k-2}$...) are removed gradually. After iteration, the gradient field is represented by:

$$\begin{gathered} \mathbf{Y}' = \mathbf{X}'\beta + \sum_{i=k+1}^{n} \varepsilon_i \\ \sum_{\mathrm{i=k+1}}^{\mathrm{n}} \varepsilon_{\mathrm{i}}^{\mathrm{T}}\mathbf{\Sigma}_{\mathrm{i}}^{-1}\varepsilon_{\mathrm{i}}^{\mathrm{T}} \approx \sigma_\xi^2\mathbf{V}_\xi \end{gathered} \tag{10}$$

where σ_ξ is near 0, and $\mathbf{V}_\xi$ is the nonsingular positive symmetric matrix. Because the influence of the outliers is removed ($\sigma_\xi \approx 0$), the orientation can be estimated by the LS method. Fig. 9 shows the result of our proposed

algorithm schematically. The ridge orientation in the sub-block is represented by the orthogonal direction to the line shown in (b) and (c). The line in (b) is pulled by the outliers caused by the scar. After removing the outliers in the gradient field, the line in (c) represents the reliable direction.

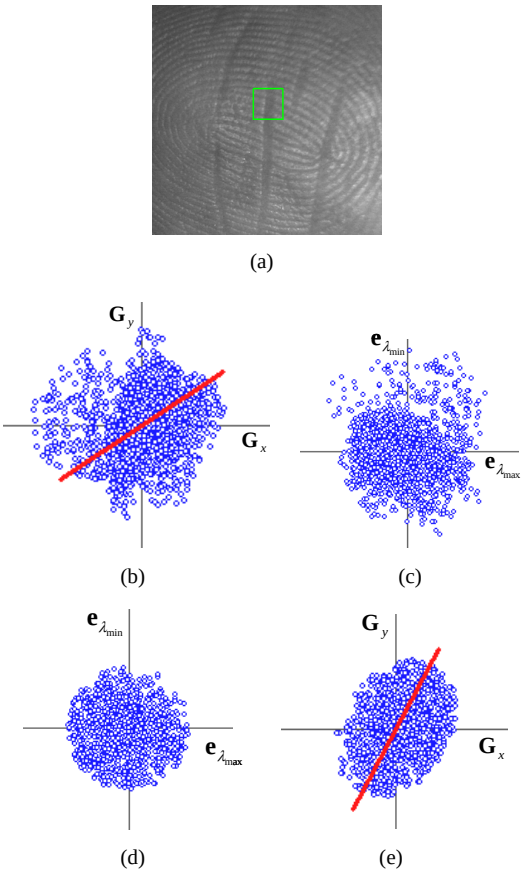

Fig. 9. (a) A sub-block image (b) A 2D gradient field with outliers (c) A whitened 2D gradient field (d) A whitened 2D gradient field without outliers (e) A 2D gradient field without outliers

IV. Fingerprint Quality Evaluation

The performance of the fingerprint recognition system is very sensitive to the quality of the captured fingerprint images. It is therefore desirable to estimate the quality of a fingerprint image before extracting fingerprint minutiae. There are a number of techniques to estimate the quality of a fingerprint image [15][16][17][18].

In images captured by mobile cameras, there are three factors which lead to poor quality: weak contrast caused by the incorrect location of the camera's depth of field (Dof) and the finger, fingerprint scars, and fingerprint abrasion. Fig. 10 shows an image that demonstrates bad quality regions. We classify good quality regions and bad quality regions by using consistent orientation in the gradient field where noise has been removed.

A. Quality Measurement

A fingerprint image within a small region generally consists of a similar orientation pattern. Therefore, consistent orientation can be a distinguishable feature between good and bad quality regions. The consistent orientation of a sub-block is measured by the ratio of eigen-values in the image gradient field, (which is called coherence) as follows[7]:

$$Coherence = \frac{\lambda_{\max} - \lambda_{\min}}{\lambda_{\max} + \lambda_{\min}} = \frac{\sqrt{(G_{xx} - G_{yy})^2 + 4G_{xy}^2}}{G_{xx} + G_{yy}} \quad (11)$$

where $\lambda_{\max}$ and $\lambda_{\min}$ are the first and second eigen-values and $\begin{bmatrix} G_{xx} & G_{xy} & G_{yy} \end{bmatrix}$ is $\begin{bmatrix} \sum_w G_x^2 & \sum_w G_x G_y & \sum_w G_y^2 \end{bmatrix}$. It is obvious that there is coherence between 0 and 1. The larger the value, the stronger the consistent orientation. Because coherence is measured based on the gradient field, it is sensitive to noise. To dampen the influence of the noise, we measure the coherence in the gradient field where noise is removed. The gradient field is obtained by the iterative robust regression method discussed in section 4. The overall flowchart of orientation estimation and quality evaluation is shown in Fig. 11. After estimating the orientation, the gradient field where the outliers are removed is created, and the proposed quality measurement is calculated in the gradient field.

V. Experimental Results

A set of fingerprint images was acquired with a mobile fingerprint sensor, similar to that used in a 1-megapixel camera. The finger was positioned at about 5cm in front of the sensor to obtain a clear finger image. The captured finger images were 24-bit color images with a resolution of 640×512.

A. Segmentation

600 test images were evaluated in terms of segmentation. Each test image was manually divided into the fingerprint region and the background region. Table 1 shows the results of fingerprint segmentation. The rate is computed by the ratio of the manually defined blocks (true) and the decided blocks (result) by the algorithm in 8×8 block bases.

TABLE I
Segmentation Result

True \ Result	Fingerprint Region	Background Region
Fingerprint Region	98.06%	1.94%
Background Region	0.04%	99.96%

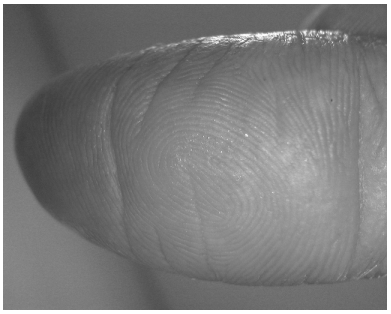

Fig. 10. A fingerprint image with bad quality regions

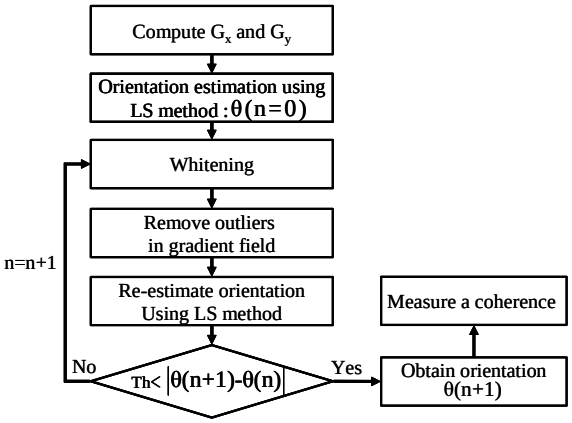

Fig. 11. The overall procedure of orientation estimation and quality evaluation

B. Orientation

We compare the proposed approach with the conventional gradient-based approach. Fig. 12 gives an example for comparison, where (a) is the original image, (b) is the orientation field estimated by the conventional gradient-based approach, and (c) is the result of the proposed approach. In Fig. 12, region A (shown by the circle) is affected by a scar, and region B (shown by the dotted circle) is affected by weak contrast. While there is no reliable orientation information when using the conventional approach, the proposed approach produces robust orientation information in regions A and B. In the other region, the conventional and proposed approaches produce the same result because the influence of the outliers is small in that region.

C. Quality check

To evaluate the proposed fingerprint quality check algorithm, we compare the proposed method with existing quality checking methods by measuring the separability between the good quality regions and the bad quality regions. The existing methods are the directional information method [15], the WSQ-based method [16], the Gabor filter-based method[17], and the conventional coherence method [18]. To define the good quality regions and the bad quality regions, we divided the minutiae into true minutiae and false minutiae manually for 100 independent fingerprint images which were acquired with a mobile camera. The good quality regions were defined with small blocks including true minutiae, and the bad quality regions were defined with small blocks including false minutiae. Fig. 13 shows the true minutiae and false minutiae. Fig. 14 shows the distribution between the good quality regions and the bad quality regions obtained from 100 fingerprint images, and Table 2 shows the separability of each distribution. These clearly show that the distribution when using the proposed method is more separable than when using existing methods.

D. Verification Performance

To evaluate verification performance, we implemented a minutia extraction [19] and a matching algorithm [20]. After

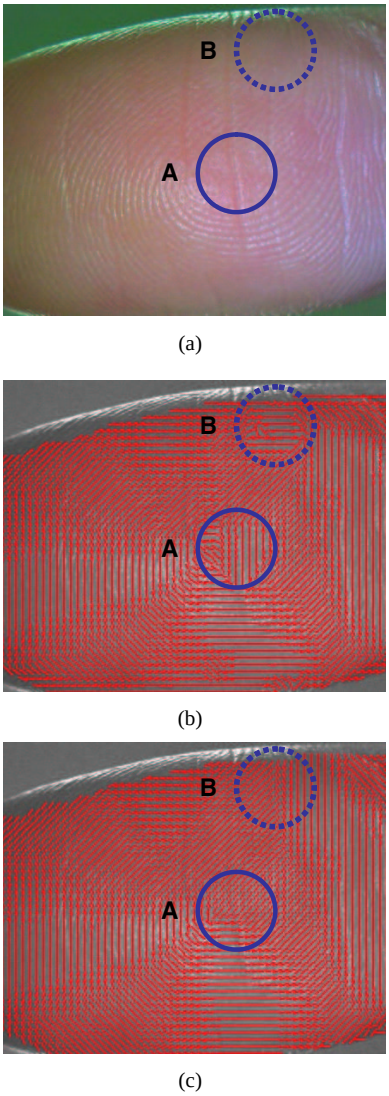

Fig. 12. Comparison between the gradient-based method and the proposed method (a) Original image (b) Result of the gradient-based method (c) Result of the proposed method.

fingerprint segmentation, orientation estimation, and quality evaluation using the proposed algorithms, the gray-value fingerprint image was enhanced using Gabor filters. During the enhancement process, the fingerprint image was binarized for thinning, and minutiae were extracted from the thinning fingerprint images. Finally, a matching algorithm was adopted from [20] to compare an input fingerprint and a template. Fig. 15 shows the resulting images of the minutia extraction. In this experiment, we used a fingerprint database of 840 fingerprint images from 168 different fingers with 5 fingerprint images for each finger. Fig. 16 shows the matching results with the ROC in order to compare the proposed preprocessing algorithm with existing algorithms. The existing preprocessing algorithms are described in Table 3. From this experiment, we can observe that the performance of the fingerprint verification system is significantly improved when our fingerprint preprocessing is applied to the input fingerprint images.

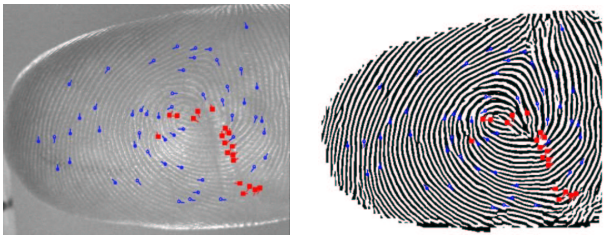

(a) (b)

Fig. 13. Minutiae points of manually-defined quality (a) Original image (b) Enhanced binary image (Rectangular:False minutiae, Circle:True Minutiae)

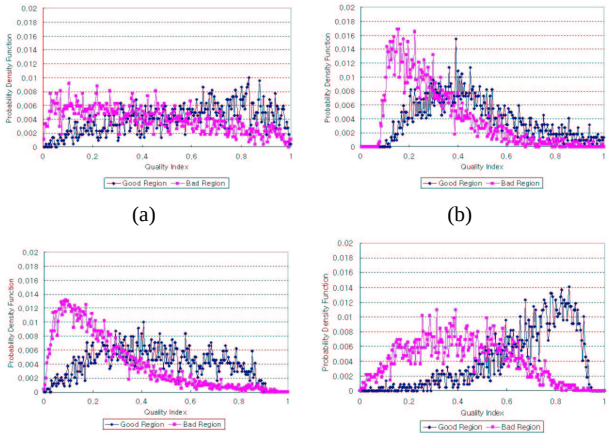

(a) (b) (c) (d)

Fig. 14. Probability density function of each type of quality measurement (a) WSQ (b) Gabor filter (c) Coherence (d) The proposed method

VI. Conclusions

In this paper, a fingerprint preprocessing algorithm using a mobile camera was proposed. Since the characteristics of fingerprint images acquired with a mobile camera are quite different from those obtained by conventional touch-based sensors, a new fingerprint preprocessing algorithm was used. The main contributions of this paper are: (i) a fingerprint segmentation algorithm, (ii) a robust orientation estimation algorithm, and (iii) a new measurement for fingerprint quality evaluation based on consistent orientation. To segment the fingerprint regions from the background regions, we investigated the color information, texture information and size information of the fingerprint images. Based on our experimental results, the proposed segmentation algorithm produced excellent performance. In the orientation estimation algorithm, because mobile cameras produce more noise than conventional sensors, we proposed a new orientation estimation algorithm that is robust to outliers. The proposed method removed the gradient elements corresponding to outliers iteratively and the dominant orientation was estimated by the LS method. For quality evaluation, we developed a new fingerprint quality measurement method based on consistent orientation. Consistent orientation was measured in a gradient field where noise was removed. The experimental results clearly showed that our fingerprint verification system demonstrated enough verification performance to be applied to mobile security devices.

TABLE II

The separability of each type of quality measurement(Separability $= \frac{|\mu_{\text{Good}} - \mu_{\text{Bad}}|}{\sqrt{\left(\sigma^2_{\text{Good}} + \sigma^2_{\text{Bad}}\right)/2}}$)

Quality Measurement	Separability
WSQ	0.751
Gabor filter	0.843
Coherence	1.553
Proposed method	1.754

(a) (b) (c) (d)

Fig. 15. The resulting images of minutiae extraction with color fingerprint images: (a) Fused gray-value image (b) Enhanced image (c) Thinning image (d) Minutiae extraction

VII. Acknowledgment

This work was supported by Korea Science and Engineering Foundation (KOSEF) through the Biometrics Engineering Research Center at Yonsei University.

References

[1] W. Skarbek, A. Koschan, "Colour image segmentation - a survey", Technical Report, Tech. Univ. of Berlin, October 1994.
[2] HD Cheng, XH Jiang, Y. Sun, and J. Wang, "Color image segmentation: advances and prospects", Pattern Recognition 34 (12) (2001) 2259-2281.
[3] E. Salari, and Z. Ling, "Texture Segmentation Using Hierarchical Wavelet Decomposition", Pattern Recognition, Vol.23, No.12, pp.1819-1824, 1995.
[4] Trygve Randen, John H? Husły, "Filtering for Texture Classification: A Comparative Study", IEEE Transactions on PAMI, v.21 n.4, p.291-310, April 1999.
[5] Michael Kass, Andrew Witkin,"Analyzing oriented pattern", Computer Vision, Graphics, and Image Processing, Vol. 37, Issue 3, pp. 362-385, 1987.
[6] Nalini K.; Ratha; Chen Shaoyun; Anil K. Jain; "Adaptive flow orientation-based feature extraction in fingerprint images", Pattern Recognition, Volume 28, Issue 11, November 1995, Pages 1657-1672
[7] A.M. Bazen and S.H. Gerez, "Directional field computation for fingerprints based on the principal component analysis of local gradients", in Proceedings of ProRISC2000, 11th Annual Workshop on Circuits, Systems and Signal Processing, Veldhoven, The Netherlands, Nov. 2000.
[8] X. G. Feng and P. Milanfar, "Multiscale principal components analysis for image local orientation estimation", The 36th Asilomar Conference on Signals, Systems and Computers, vol.1, pp.478-482, 2002.
[9] P. Vizcaya and L. Gerhardt, "A nonlinear orientation model for global descript-ion of fingerprints," Pattern Recognition, vol. 29, no.7, pp.1221-1231, 1996.
[10] Jie Zhou, Jinwei Gu, "A model-based method for the computation of fingerprints' orientation field", IEEE Transactions of image processing, vol.13, No.6, pp.821-835, 2004
[11] Bamberger, R.H., Smith, M.J.T, "A multirate filter bank based approach to the detection and enhancement of linear features in images", Acoustics, Speech, and Signal Processing, 1991. ICASSP-91, 1991 International Conference on , vol.4, pp. 2557 -2560, 1991
[12] K.V. Mardia, A.J. Baczkowski, X. Feng, T.J. Hainsworth, "Statistical methods for automatic interpretation of digitally scanned fingerprints", Pattern Recognition Letters, Volume 18, Issues 11-13, November 1997, Pages 1197-1203
[13] Douglas C. Montgomery, Elizabeth A. Peck, G. Geoffrey Vining, "Introduction to Linear Regression Analysis, 3rd Edition", John Wiley Sons. Inc. 2001.

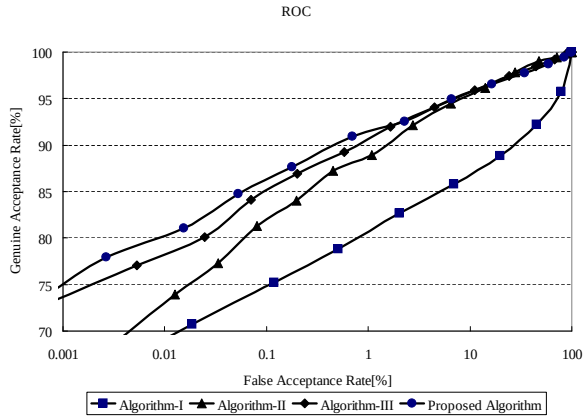

Fig. 16. Receiver Operating Curves(ROC); the ROC shows the improvement in verification performance using the preprocess algorithm

TABLE III

THE EXISTING ALGORITHM

Algorithm	Segmentation	Orientation	Quality
I	Proposed method	Gradient Based	WSQ based
II			Gabor filter based
III			Coherence Based

[14] A. Hyvärinen, J. Karhunen, E. Oja, ”Independent component Analysis”, John Wiley Sons. Inc, 2001

[15] Bolle et al, ”System and method for determining the quality of fingerprint images”, United State Patent number, US5963656, 1999

[16] Nalini K. Ratha, Ruud Bolle, ”Fingerprint Image Quality Estimation”, IBM Computer Science Research Report RC21622, 1999

[17] L.L.Shen, A. Kot and W.M Koo, ”Quality Measures of Fingerprint Images”, 3rd International Conference AVBPA 2001, p182-271, June 2001

[18] Eyung Lim, Xudong Jiang, Weiyun Yau,”Fingerprint quality and validity analysis”, Image Processing. 2002. Proceedings. 2002 International Conference on, vol.3, pp.469-472, 2002.

[19] L. Hong, Y. Wan and A.K. Jain, ”Fingerprint Image Enhancement: Algorithms and Performance Evaluation”, IEEE Transactions on PAMI, Vol. 20, No. 8, pp.777-789, August 1998.

[20] D. Lee, K. Choi and Jaihie Kim, ”A Robust Fingerprint Matching Algorithm Using Local Alignment”, International Conference on Pattern Recognition, Quebec, Canada, August 2002.